

# Type II toxin/antitoxin MqsR/MqsA controls type V toxin/antitoxin GhoT/GhoS

Xiaoxue Wang,<sup>1\*\*</sup> Dana M. Lord,<sup>2</sup> Seok Hoon Hong,<sup>4</sup> Wolfgang Peti,<sup>2</sup> Michael J. Benedik,<sup>5</sup> Rebecca Page<sup>3</sup> and Thomas K. Wood<sup>4,5,6,7\*</sup>

<sup>1</sup>Key Laboratory of Marine Bio-Resources Sustainable Utilization, South China Sea Institute of Oceanology, Chinese Academy of Sciences, Guangzhou, China.

Departments of <sup>2</sup>Molecular Pharmacology, Physiology, and <sup>3</sup>Molecular Biology, Cell Biology and Biochemistry, Brown University, Providence, RI, USA.

Departments of <sup>4</sup>Chemical Engineering and <sup>5</sup>Biology, Texas A&M University, College Station, TX, USA.

Departments of <sup>6</sup>Chemical Engineering and

<sup>7</sup>Biochemistry and Molecular Biology, Pennsylvania State University, University Park, PA, USA.

## Summary

**Toxin endoribonucleases of toxin/antitoxin (TA) systems regulate protein production by selectively degrading mRNAs but have never been shown to control other TA systems. Here we demonstrate that toxin MqsR of the MqsR/MqsA system enriches toxin *ghoT* mRNA *in vivo* and *in vitro*, since this transcript lacks the primary MqsR cleavage site 5'-GCU. GhoT is a membrane toxin that causes the ghost cell phenotype, and is part of a type V TA system with antitoxin GhoS that cleaves specifically *ghoT* mRNA. Introduction of MqsR primary 5'-GCU cleavage sites into *ghoT* mRNA reduces ghost cell production and cell death likely due to increased degradation of the altered *ghoT* mRNA by MqsR. GhoT also prevents cell elongation upon the addition of low levels of ampicillin. Therefore, during stress, antitoxin GhoS mRNA is degraded by toxin MqsR allowing *ghoT* mRNA translation to yield another free toxin that forms ghost cells and increases persistence. Hence, we show that GhoT/GhoS is the first TA system regulated by another TA system.**

## Introduction

Bacterial toxin/antitoxin (TA) systems play prominent roles in cell physiology including altruistic behaviour such as phage inhibition (Pecota and Wood, 1996), global gene regulation (Wang and Wood, 2011) and tolerance to antibiotics (Lewis, 2010). For antitoxins, both MqsA (Wang *et al.*, 2011) and DinJ (Hu *et al.*, 2012) have been shown to repress the stationary-phase sigma factor RpoS and thereby influence the response to stress and biofilm formation as global regulators. Toxins in TA systems also play a role in gene regulation in that mRNA endoribonuclease toxins cleave specific mRNAs and thereby cause differential mRNA decay (Wang and Wood, 2011). For example, upon antibiotic stress, toxin MazF degrades most mRNAs with ACA sequences, but its activity also results in the preferential synthesis of a subset of small proteins whose mRNAs are not degraded (Amitai *et al.*, 2009). These enriched proteins are necessary both for toxicity and for survival (Amitai *et al.*, 2009). Therefore, both toxins and antitoxins may be considered global regulators.

The endoribonuclease toxin MqsR (motility quorum sensing regulator) (Ren *et al.*, 2004; González Barrios *et al.*, 2006; Brown *et al.*, 2011) of the MqsR/MqsA TA system is also a global regulator (González Barrios *et al.*, 2006; Kim *et al.*, 2010). It cleaves specific mRNA primarily at 5'-GCU sites (Yamaguchi *et al.*, 2009; Christensen-Dalsgaard *et al.*, 2010) and leads to enrichment of mRNAs that code for stress-associated proteins CstA, CspD, RpoS, Dps and HokD (Kim *et al.*, 2010). The binding of MqsR to its antitoxin MqsA potentially inhibits MqsR toxicity (Brown *et al.*, 2011).

MqsR/MqsA is a type II TA system (protein toxin inhibited by the binding of a protein antitoxin), and type II TA systems are one of the most widespread forms of TA systems (Hayes and Van Melder, 2011). In type I TA systems (RNA–RNA), the antitoxin RNA prevents the translation of toxin RNA through complementary base pairing (Hayes and Van Melder, 2011), in type III TA systems (RNA–protein), the antitoxin RNA inhibits the protein toxin (Hayes and Van Melder, 2011), in type IV TA systems (protein–protein), the protein antitoxin interferes with binding of the toxin to its target (Masuda *et al.*, 2012), and in type V systems (protein–RNA), the antitoxin is a specific RNase that cleaves the toxin mRNA (Wang *et al.*, 2012).

Received 25 October, 2012; revised 28 November, 2012; accepted 29 November, 2012. For correspondence. \*E-mail tuw14@psu.edu; Tel. (+1) 814 863 4811; Fax (+1) 814 865 7846; \*\*E-mail xxwang@scsio.ac.cn; Tel. (+86) 20 89235460; Fax (+86) 20 89267515.

There are 14 *Escherichia coli* mRNA transcripts that do not contain the *MqsR*-preferred 5'-GCU cleavage site, and six of these (*pheL*, *tnaC*, *trpL*, *yciG*, *ygaQ* and *ralF*) are differentially regulated in biofilms (Domka *et al.*, 2007). One of these 14 transcripts that lacks 5'-GCU sites is *ghoT* [*yjdO*, *ghost* cells (Wang *et al.*, 2012)]. *GhoT* is a membrane toxin that produces the ghost-cell phenotype (lysed cells with damaged membranes) (Wang *et al.*, 2012). The antitoxin for *GhoT*, *GhoS*, cleaves specifically *ghoT* mRNA thereby halting *ghoT* expression; hence, this TA system is the first type V system in that an enzyme antitoxin inactivates the mRNA of the toxin (Wang *et al.*, 2012). The structure of antitoxin *GhoS* revealed it is related to the CRISPR-associated-2 (CAS2) sequence-specific endoribonuclease, and a whole-transcriptome study showed the specificity of *GhoS* as a ribonuclease (Wang *et al.*, 2012). Although *mqsR* is more prevalent than *ghoT*, *ghoT*-related genes are found in *Escherichia*, *Shigella*, *Salmonella*, *Citrobacter* and *Proteus* spp.

Persister cells are a small fraction of bacteria that exhibit tolerance to antibiotics without genetic change (Lewis, 2007); it is believed they survive antibiotic treatment by becoming metabolically dormant through TA systems (Lewis, 2010). The evidence relating TA systems to persistence includes the finding that when *MqsR* is inactivated, persister cell formation is reduced (Kim and Wood, 2010); production of *MqsR* also increases persistence. Similarly, deletion of the *TisB* toxin of the *TisAB/IstR-1* type I TA system decreases persistence (Dörr *et al.*, 2010). Subsequent studies have also demonstrated the importance of TA systems for persistence by showing that cells lacking 10 mRNA endoribonuclease toxins including *MqsR* form less persister cells (Maisonneuve *et al.*, 2012). In persister cells, *mqsR* is also the most induced gene (Shah *et al.*, 2006).

Our previous studies showed that the antitoxin *MqsA* is rapidly degraded by Lon protease which frees toxin *MqsR* upon stress (Wang *et al.*, 2011). The importance of Lon for persister cell formation has been demonstrated by showing both that cells lacking *lon* have reduced persister cell formation and that removal of the 10 toxins causes the *lon* mutant to no longer affect persistence (Maisonneuve *et al.*, 2012).

We hypothesized that since *ghoT* mRNA lacks the primary *MqsR* 5'-GCU sites, it would be enriched under conditions when *MqsR* is produced. Here we demonstrate that *MqsR* does enrich *ghoT* transcripts and thereby activates expression of this membrane toxin which is involved in persister cell formation.

## Results

### *MqsR* requires *GhoT* to prevent cell elongation

Previously, we examined the 14 *E. coli* transcripts that lack 5'-GCU sites to determine if these transcripts were

related to the ability of *MqsR* to increase persistence (Wang *et al.*, 2012). Among them, deleting gene *ghoT* had one of the largest negative effects on *MqsR*-mediated persistence; corroborating this result, production of *GhoT* increased persistence 48-fold (Wang *et al.*, 2012). We repeated these persister experiments by varying the ampicillin concentration and found similar results at both 35  $\mu\text{g ml}^{-1}$  and 100  $\mu\text{g ml}^{-1}$  ampicillin for *MqsR* production in the wild-type and in the *ghoT* mutant so the results are not influenced by the antibiotic concentration. In addition, we determined that the minimum inhibitory concentration for ampicillin was the same for both strains (approximately 5  $\mu\text{g ml}^{-1}$ ). Hence, we investigated further the relationship between *MqsR* and *GhoT* in *E. coli* to determine how *GhoT* influences persister cell formation when *MqsR* is produced.

To initially probe the relationship between *MqsR* and *GhoT*, we used microscopy. High concentrations of ampicillin (100  $\mu\text{g ml}^{-1}$ ) are commonly used to assess persister cell formation in *E. coli* (Balaban *et al.*, 2004; Keren *et al.*, 2004; Shah *et al.*, 2006; Kim *et al.*, 2010). When added at 100  $\mu\text{g ml}^{-1}$ , ampicillin rapidly lyses non-persister cells, which makes it difficult to probe for changes in cell morphology; hence, here we used a lower ampicillin concentration (20  $\mu\text{g ml}^{-1}$ ), which causes cell elongation rather than lysis allowing for the observation of the response to  $\beta$ -lactam antibiotics (Rolinson, 1980). We reasoned that since *MqsR* increases persister cells (Kim and Wood, 2010), *MqsR* should prevent cells from elongating upon addition of ampicillin since these persisters would be tolerant of the antibiotic. As expected, we found that addition of 20  $\mu\text{g ml}^{-1}$  ampicillin to wild-type cells (BW25113/pCA24N) caused cell elongation of most cells (23  $\pm$  3  $\mu\text{m}$ ) after 4 h by inhibiting cell division (Donachie and Begg, 1970; Staugaard *et al.*, 1976), and bulges or collars were observed at the division site (red arrows in Fig. 1A) as reported by others (Donachie and Begg, 1970; Rolinson, 1980). After 10 h, the majority of the cells lysed (Fig. 1A, left panel). In contrast, the majority of cells producing *MqsR* (BW25113/pCA24N-*mqsR*) were not elongated (1.5  $\pm$  0.6  $\mu\text{m}$ ) after 4 h with ampicillin, and the cells remained intact with sizes increased moderately after 10 h (3.5  $\pm$  0.9  $\mu\text{m}$ ) (Fig. 1A, middle panel). This dramatic increase in persister cells is due to production of the toxin *MqsR*. For cells producing *MqsR* in the absence of *ghoT* ( $\Delta$ *ghoT*/pCA24N-*mqsR*), a few cells were significantly elongated after 4 h with ampicillin, and the majority of cells were significantly elongated after 10 h (38  $\pm$  7  $\mu\text{m}$ ) (Fig. 1A, right panel). Hence, *MqsR* prevents cell elongation upon the addition of ampicillin primarily via its control of *GhoT*.

We also investigated how cells, with or without *GhoT*, respond to ampicillin challenge. After 4 h with 20  $\mu\text{g ml}^{-1}$  ampicillin, cells producing *GhoT* ( $\Delta$ *ghoT*/pCA24N-*ghoT*)

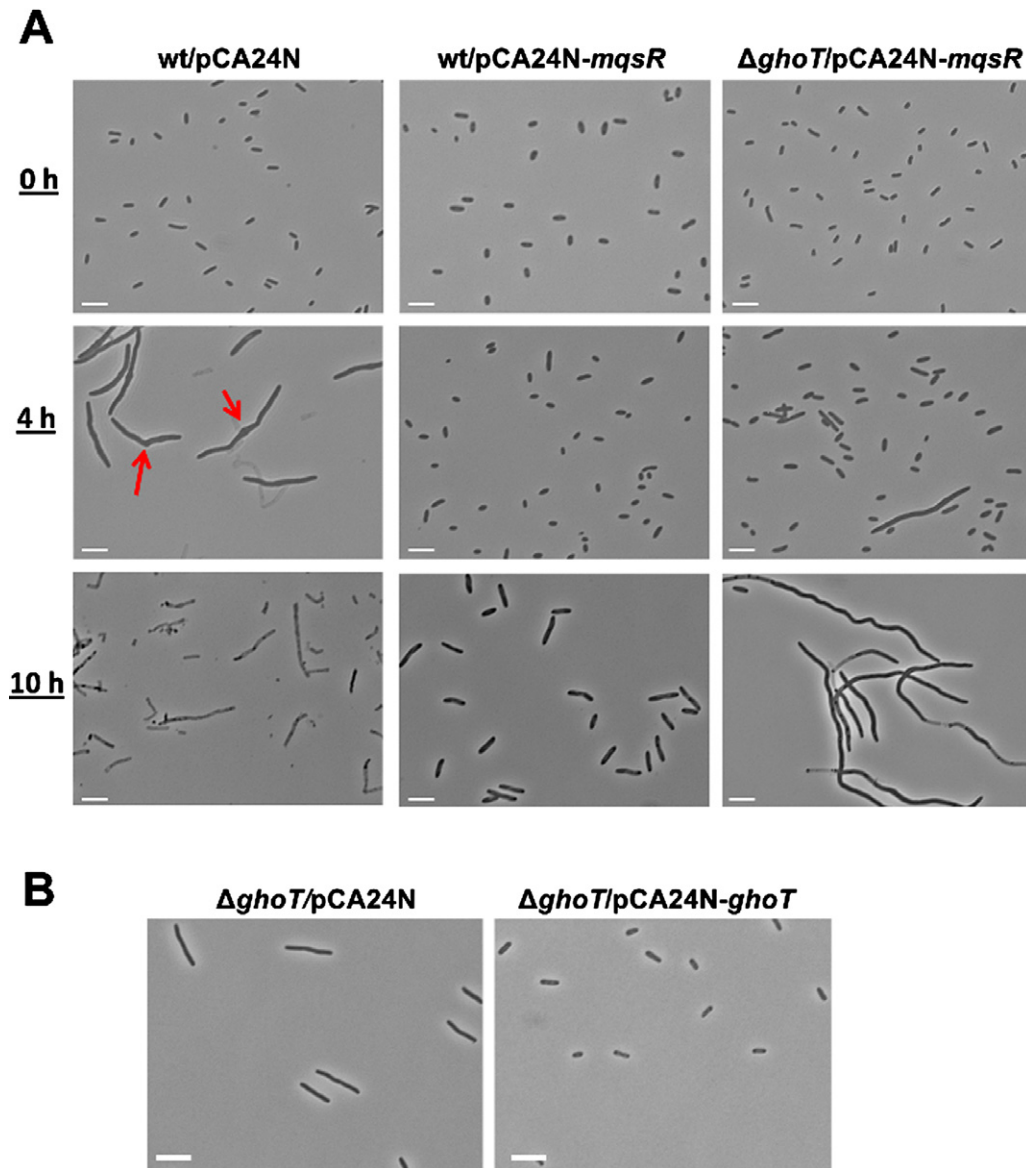


**Fig. 1.** GhoT decreases cell size in the presence of ampicillin.

A. Cell morphology after 0 h, 4 h and 10 h with ampicillin ( $20 \mu\text{g ml}^{-1}$ ) for cells producing MqsR (wt/pCA24N-*mqsR*) and cells producing MqsR but without *ghoT* ( $\Delta$ *ghoT*/pCA24N-*mqsR*). Red arrows point to the bulges or collars with ampicillin.

B. Cell morphology after 4 h with ampicillin ( $20 \mu\text{g ml}^{-1}$ ) for cells without GhoT ( $\Delta$ *ghoT*/pCA24N) and cells with GhoT ( $\Delta$ *ghoT*/pCA24N-*ghoT*). Two independent cultures of each strain were evaluated and representative images were shown. Scale bars indicate  $5 \mu\text{m}$ .

were not elongated ( $1.7 \pm 0.5 \mu\text{m}$ ) whereas those that lacked GhoT ( $\Delta$ *ghoT*/pCA24N) were elongated ( $5 \pm 1 \mu\text{m}$ ) (Fig. 1B). Note that normal cells prior to antibiotic treatment were about  $1.8 \mu\text{m}$ . This result corroborates that GhoT prevents cell elongation with ampicillin stress. Since persister cells are not dividing and are metabolically dormant with smaller sizes than non-persister cells when exposed to bactericidal antibiotics including ampicillin (Lewis, 2010), these micrographs provide additional evidence that MqsR helps to maintain a dormant

state in the presence of ampicillin through GhoT action and that deletion of *ghoT* reduces the ability of MqsR to maintain persistence.

#### *MqsR regulates production of GhoT in vivo through differential ghoS mRNA decay*

Given the link between MqsR and GhoT, we investigated *in vivo* whether MqsR can regulate *ghoST* mRNA stability at a post-transcriptional level by using quantitative real-

**Table 1.** Oligonucleotides used for RT-PCR, qRT-PCR, mutant verification, site-directed mutagenesis (target mutated nucleotides are underlined) and *in vitro* transcription (for the forward primers, the T7 promoter sequence is underlined and the bases of the promoter sequence incorporated into RNA during transcription are in bold).

Purpose/name	Sequence (5' to 3')
RT-PCR and qRT-PCR	
<i>ghoS</i> -f	CCATCATCTTATTCCTCAGTGTCT
<i>ghoS</i> -r	TAAGTCTAAGCATTGAGCCTGATT
<i>ghoT</i> -f	TGGTGTGAACATATCCTTTGTCA
<i>ghoT</i> -r	TAATGCCACAGGCAGACTCA
<i>ralR</i> -f	AAACCATGTCCATTTTGTGGT
<i>ralR</i> -r	TCCAGTGGTTCGTTTATTCCA
<i>ompA</i> -f	CACTGGCTGGTTTCGCTACCG
<i>ompA</i> -r	ACCCATTTCAAAGCCAACATC
<i>ompF</i> -f	AAGCGCAATATTCTGGCAGT
<i>ompF</i> -r	TGCCACCGTAAGTGTTC
<i>yciG</i> -f	ACATCGTGGTTCAGGAA
<i>yciG</i> -r	TACCACCGCTTTGTTGACCG
Deletion mutant verification	
<i>GhoS</i> -veri-f	CTCCTATATGAGAATCATCAATCGGGG
<i>GhoS</i> -veri-r	GACAAAGGATATGTTACACCAATCAC
<i>GhoT</i> -veri-f	GACCTCAACATTATGACAGTTGATGAC
<i>GhoT</i> -veri-r	GCTTCGTTTCATCGTTCCGCAAATCCAG
Site-directed mutagenesis	
<i>GhoT</i> -GCU-1-f	GTGATTGGTGTGAACATAAGCTTTGTCATTATCTGGTTTATCTC
<i>GhoT</i> -GCU-1-r	GAGATAAACAGATAATGACAAAGCTTATGTTACACCAATCAC
<i>GhoT</i> -GCU-2-f	CACATATTCGTTTACTTAGTGCTTTCTGGTCGGAATAACCTGG
<i>GhoT</i> -GCU-2-r	CCAGGTTATTCGACCAGGAAAGCCTAAGTAAACGAATATGTG
T7 <i>in vitro</i> transcription	
PT7- <i>GhoT</i> -f	TAATACGACTCACTATA <b>AGGGAGA</b> ATGGCACTATTCTCTAAAATATTAATTTTT
PT7- <i>GhoT</i> -r	CTAAAAGAGAGAAAAAGTAATGC
PT7- <i>GhoS</i> -f	TAATACGACTCACTATA <b>AGGGAGA</b> ATGGAAGGTAAAACAAGTTCAATACTTAT
PT7- <i>GhoS</i> -r	TCATCAACTGTCATAATGTTGAG

f indicates forward primer and r indicates reverse primer.

time reverse transcription PCR (qRT-PCR) using a primer pair within the coding portion of each gene (Table 1). We found that when *MqsR* was produced [BW25113/pBS(Kan)-*mqsR* versus BW25113/pBS(Kan)], there was

a 5 ± 1-fold increase in the 3' *ghoT* portion of the *ghoST* mRNA compared with the 5' *ghoS* portion, which suggests that the *ghoST* transcript is preferentially degraded at the 5' end when *MqsR* is active (Table 2 lists the qRT-PCR

**Table 2.** Summary of the qRT-PCR results.

Conditions	Target mRNA	Fold change	5'-GCU site
BW25113/pBS(Kan)- <i>mqsR</i> versus BW25113/pBS(Kan) 1 mM IPTG for 60 min	<i>ghoT</i>	40 ± 1	0
	<i>ghoS</i>	8 ± 1	3
	<i>ompA</i>	-4.5 ± 1	27
	<i>ompT</i>	3 ± 2	14
	<i>ompF</i>	-2 ± 1	20
	<i>kilR</i>	10.8 ± 0.4	0
	<i>ralR</i>	12 ± 1	0
	<i>yciG</i>	11 ± 1	0
BW25113 wild-type 2 µg ml <sup>-1</sup> nalidixic acid for 90 min versus no nalidixic acid	<i>mqsR</i>	18 ± 2	1
	<i>ghoT</i>	40 ± 1	0
	<i>ompA</i>	1 ± 1	27
BW25113 wild-type 10 µg ml <sup>-1</sup> azlocillin for 90 min versus no azlocillin	<i>mqsR</i>	20 ± 2	1
	<i>ghoT</i>	48 ± 2	0
	<i>ompA</i>	-1 ± 1	27
BW25113 wild-type 20 mM H <sub>2</sub> O <sub>2</sub> for 5 min versus no H <sub>2</sub> O <sub>2</sub>	<i>mqsR</i>	4.6 ± 0.6	1
	<i>ghoT</i>	6 ± 2	0

Experimental conditions and the target mRNA are indicated along with the number of 5'-GCU sites in the target mRNA. The fold changes indicate the changes in enrichment (not necessarily changes in transcription) after differential mRNA decay by RNase *MqsR* and were calculated as described earlier (Pfaffl, 2001) relative to the housekeeping gene (*rrsG*), which was used to normalize the data. Values less than one are indicated as negative fold changes (i.e. mRNA levels were reduced relative to other mRNA). The specificity of the qRT-PCR products was verified by a melting curve analysis.



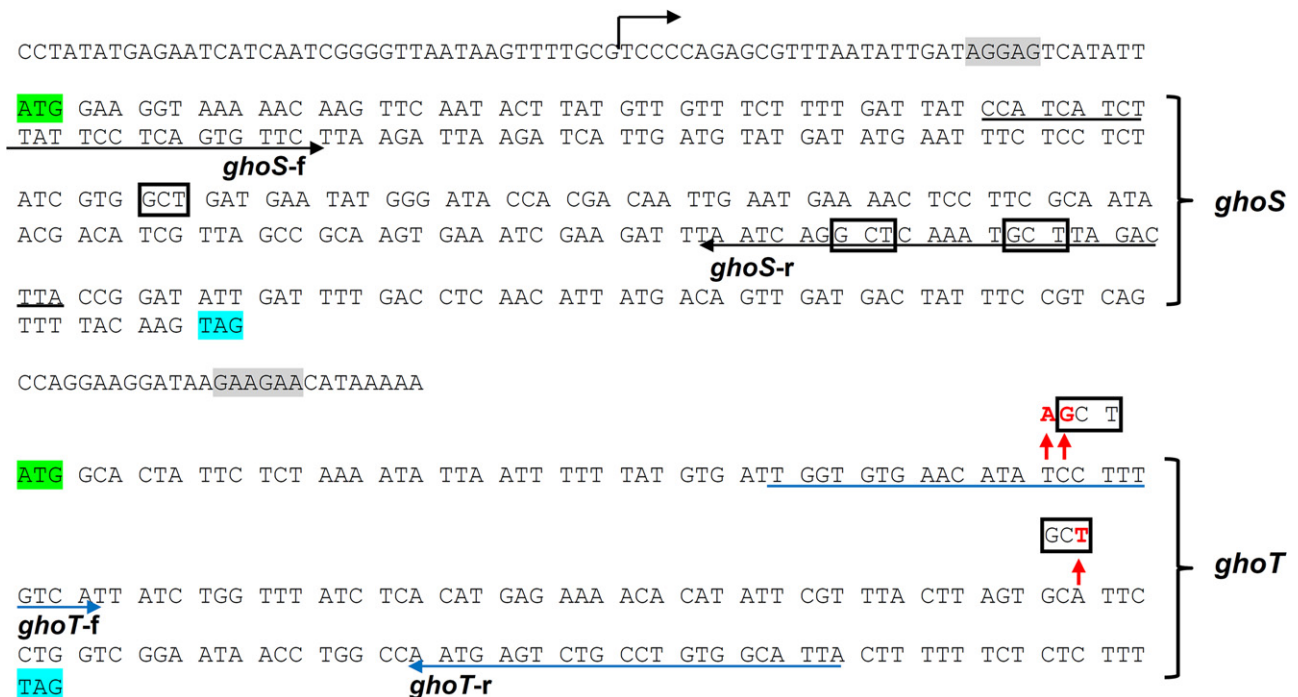


**Fig. 2.** DNA sequence of *ghoST*. The positions with introduced mutations in *ghoT* are indicated by red arrows with the changed nucleotide in red font. Native 5'-GCT sites in *ghoS* are boxed in black. Start codons are highlighted in green and stop codons are highlighted in blue. The putative transcription start site of the *ghoST* operon is indicated by a black arrow, and the putative RBS sites are highlighted in grey. Primers from *ghoS* (*ghoS-f* and *ghoS-r*) and the primers from *ghoT* (*ghoT-f* and *ghoT-r*) are underlined with their direction indicated.

results). This result is not unexpected since the region of the *ghoST* transcript that codes for *ghoS* (5' end) contains three of the primary MqsR 5'-GCU cleavage sites, whereas the region that codes for *ghoT* (3' end) does not contain any 5'-GCU cleavage sites (Fig. 2). Therefore, one mechanism by which MqsR regulates GhoT activity is by selectively degrading the *ghoST* transcript in a manner that leaves the portion of the transcript for toxin GhoT intact, while that of GhoS is degraded.

If MqsR degrades other transcripts in addition to that of *ghoS*, but not *ghoT*, *ghoT* mRNA should be enriched by comparison with these other transcripts. We investigated this using qRT-PCR (Table 2) and found that production of MqsR enriches *ghoT* mRNA  $40 \pm 1$ -fold compared with 5'-GCU-containing transcripts *ompA* (27 5'-GCU sites) and *ompF* (20 5'-GCU sites), which have been shown to be degraded by MqsR by *in vivo* and *in vitro* (Yamaguchi *et al.*, 2009), as well as *ompT* (14 5'-GCU sites). As expected, we found that three other mRNAs that lack 5'-GCU sites were enriched during production of MqsR: *killR* by  $10.8 \pm 0.4$ -fold, *raiR* by  $12 \pm 1$ -fold and *yciG* by  $11 \pm 1$ -fold. Also, ribosomal RNA *rrsG* was not affected by production of MqsR (confirmed by an intact band of 16S rRNA with agarose gel electrophoresis) since this RNA should be protected by its incorporation into ribosomes.

Similarly, we investigated *ghoT* mRNA levels under external stress conditions, where MqsR was induced at its

normal level from the chromosomal locus. Upon addition of sublethal concentrations of nalidixic acid or azlocillin to wild-type cells, *mqsR* mRNA was induced  $18 \pm 2$ -fold and  $20 \pm 2$ -fold respectively (Table 2). Under these conditions, *ghoT* mRNA was enriched by  $40 \pm 1$ -fold and  $48 \pm 2$ -fold, respectively, whereas 5'-GCU-containing *ompA* mRNA was not enriched. Upon oxidative stress (20 mM hydrogen peroxide for 5 min), due to the rapid degradation of MqsA by Lon (Wang *et al.*, 2012), *mqsR* transcription was induced  $4.5 \pm 0.6$ -fold, which, due to the increase in MqsR protein, enabled *ghoT* mRNA to increase  $6 \pm 2$ -fold. Therefore, these three stress conditions which induce *mqsR* transcription result in concomitant enrichment of *ghoT* mRNA relative to cellular mRNA.

#### *MqsR* preferentially cleaves *ghoS* mRNA in vitro

Using purified toxin MqsR, we also found that MqsR cleaves *ghoS* mRNA far more efficiently than *ghoT* mRNA (Fig. 3). The relatively small amount of degradation of native *ghoT* mRNA (Fig. 3, lane 5) appears to be related to purified MqsR cleavage at the three less favourable GCA sites based on the sizes of the fragments generated.

To further demonstrate that the lack of *ghoT* mRNA degradation was due to the absence of MqsR cleavage sites, we added two of the primary MqsR 5'-GCU cleavage sites to *ghoT* mRNA and tested whether the mutated

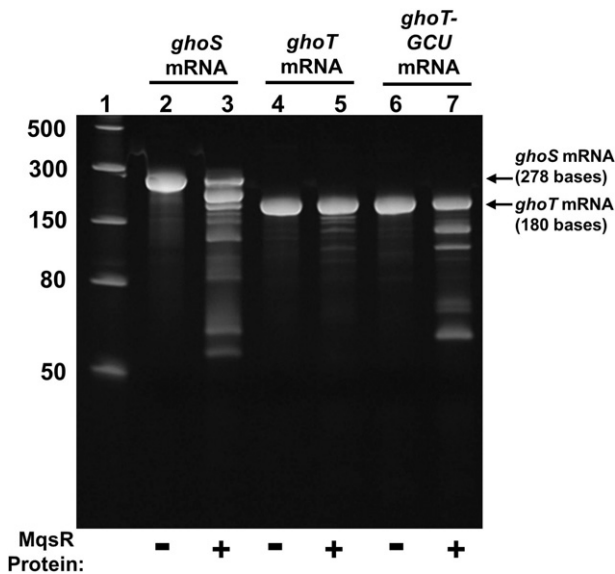


**Fig. 3.** MqsR cleaves *ghoS* mRNA more efficiently than *ghoT* mRNA *in vitro*. Two micrograms of *in vitro* synthesized *ghoS* mRNA (278 nt, lanes 2, 3), *ghoT* mRNA (180 nt, lanes 4, 5) and mutated *ghoT-GCU* mRNA with two GCU sites (180 nt, lanes 6, 7) were incubated either without (–) or with (+) 30 ng of MqsR protein for 15 min at 37°C. The arrows indicate the uncleaved *ghoS* and *ghoT* transcripts. Lane 1, low-range ssRNA ladder (sizes indicated in nt).

*ghoT-GCU* mRNA was degraded by MqsR. As it is currently unknown whether MqsR cleaves mRNA at specific bases of a codon similar to RelE, which preferentially cleaves after the second or third base of a codon (Hurley *et al.*, 2011), we introduced both a non-codon 5'-GCU and a codon 5'-GCU site into *ghoT* mRNA. Both changes are silent: at aa position 18, *TCC* (Ser) was changed to *AGC* (Ser) to create the non-codon 5'-GCU site and at aa position 37, *GCA* (Ala) was changed to *GCT* (Ala) to create a codon 5'-GCU site (Fig. 2; pCA24N-*ghoT-GCU*). Using purified toxin MqsR, we found that MqsR cleaves the mutated *ghoT* mRNA with two 5'-GCU sites (Fig. 3). Compared with the wild-type *ghoT* mRNA that lacks GCU sites, multiple cleavage products were clearly observed when the *ghoT-GCU* mRNA was used as a template. Furthermore, we also found that the sizes of the dominant cleavage products agree well with those that are predicted when the *ghoT-GCU* mRNA is cleaved at 5'-GCU sites (56, 59, 65, 115 and 121 nt) (Fig. 3, lane 7). These *in vitro* results demonstrate that MqsR preferentially cleaves 5'-GCU sequences, and that it functions without ribosomes (Yamaguchi *et al.*, 2009).

Furthermore, using a *ghoT* deletion strain (BW25113  $\Delta$ *ghoT*) to ensure that no endogenous *ghoT* transcript was produced, we found that producing MqsR resulted in threefold fewer ghost cells for those cells transformed with pCA24N-*ghoT-GCU* versus those with pCA24N-*ghoT* (Fig. 4). Live/Dead staining was also used to differentiate between cells with intact membranes (live) and cells with

damaged membranes (dead). A fourfold increase in the number of cells with intact membranes was observed in cells transformed with mutant *ghoT* DNA with two GCT (5'-GCU in the transcribed mRNA) sites (Fig. 4) as compared with wild-type *ghoT* which confirms that adding the two 5'-GCU sites decreased production of ghost cells. Therefore, both *in vitro* and *in vivo* studies demonstrate that MqsR regulates GhoT activity by GCU-dependent cleavage of *ghoS* in the *ghoST* mRNA transcript upon stress.

## Discussion

Toxin MqsR regulates toxin GhoT via post-transcriptional differential mRNA cleavage resulting in a regulatory hierarchy where one TA system controls another. The nine lines of evidence that demonstrates this are that (i) when MqsR is produced [BW25113/pBS(Kan)-*mqsR* versus BW25113/pBS(Kan)], there is a  $5 \pm 1$ -fold increase in the 3' *ghoT* portion of the *ghoST* mRNA compared with the 5' *ghoS* portion, (ii) when MqsR is produced, *ghoT* mRNA is enriched  $40 \pm 1$ -fold compared with 5'-GCU-containing transcripts *ompA* and *ompF*, which have been shown to be degraded by MqsR by *in vivo* and *in vitro* (Yamaguchi *et al.*, 2009), (iii) the addition of sublethal concentrations of nalidixic acid induces *mqsR* mRNA  $18 \pm 2$ -fold, which results in concomitant enrichment of *ghoT* mRNA  $40 \pm 1$ -fold while there is no enrichment of *ompA* mRNA, (iv) the addition of sublethal concentrations of azlocillin induces *mqsR* mRNA  $20 \pm 2$ -fold, which results in the concomitant enrichment of *ghoT* mRNA  $48 \pm 2$ -fold while there is no enrichment of the *ompA* mRNA, (v) upon oxidative stress, *mqsR* transcription was induced  $4.5 \pm 0.6$ -fold, which, in turn, enabled *ghoT* mRNA to increase  $6 \pm 2$ -fold, (vi) upon addition of two 5'-GCU sites to *ghoT* mRNA, the number of ghost cells and dead cells were reduced due to the presence of the primary cleavage sites for MqsR, (vii) MqsR cleaves more readily mutated *ghoT* mRNA with two introduced 5'-GCU sites *in vitro*, (viii) MqsR preferentially cleaves *ghoS* mRNA more efficiently than *ghoT* mRNA *in vitro*, and (ix) MqsR-derived persistence depends on GhoT activity. Although it is possible that other endoribonuclease toxins might also impact the stability of *ghoST* mRNA under stressed conditions *in vivo*, the *in vitro* studies demonstrate the importance of toxin MqsR on the stability of *ghoST* mRNA. Therefore, MqsR is the first identified toxin that regulates a second TA system, GhoT/GhoS, illustrating how MqsR, along with MqsA (Wang *et al.*, 2011), function as global regulators of environmental stress in *E. coli*. These results also illustrate how cells have interwoven TA systems into their genetic fabric to control cell physiology.

Our model of the response of *E. coli* to oxidative stress, as mediated by the MqsR/MqsA and GhoT/GhoS TA

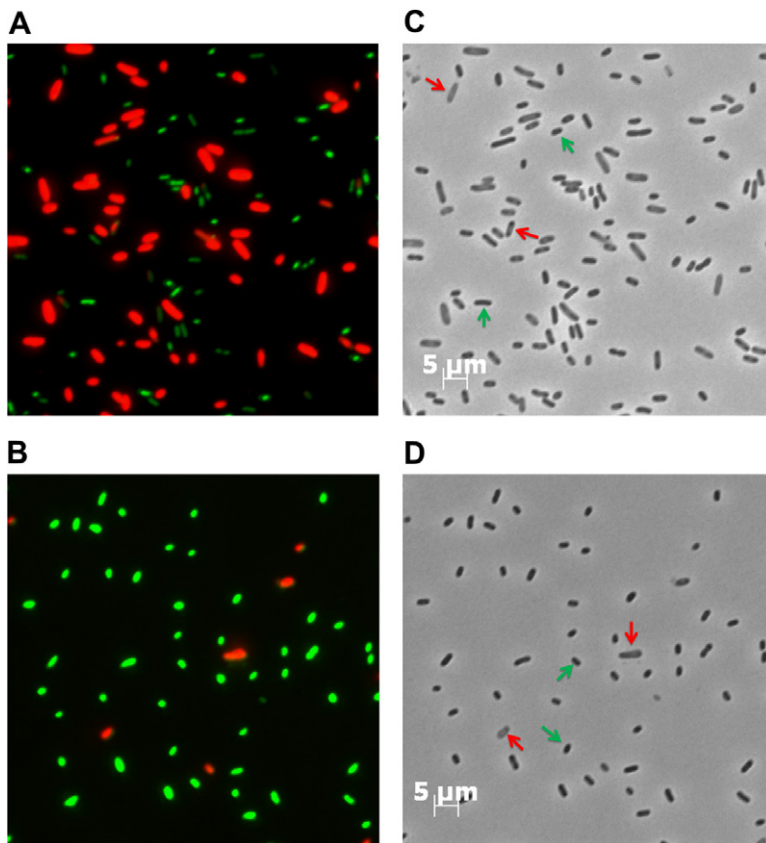


**Fig. 4.** Addition of 5'-GCU to *ghoT* mRNA reduces MqsR toxicity. Live/dead staining via fluorescence microscopy showing that the production of wild-type GhoT (A) causes ghost cell morphology and leads to cell death (red), while production of mutant *ghoT* mRNA (containing two introduced 5'-GCU sites) (B) has less ghost cells and less cell death (live cells are green). Panels (C) and (D) show the corresponding phase-contrast microscopy images. Red arrows indicate representative ghost cells, and green arrows indicate representative live cells. Images were taken 3 h after the addition of 0.5 mM IPTG to cultures of  $\Delta ghoT$   $\Delta Km/pBS(Kan)-mqsR/pCA24N-ghoT$  (A and C) and  $\Delta ghoT$   $\Delta Km/pBS(Kan)-mqsR/pCA24N-ghoT-GCU$  (B and D) when the turbidity reached 0.5, which allows production of MqsR through its leaky  $P_{lac}$  promoter followed by the production of GhoT through its  $P_{T5-lac}$  promoter. Two independent cultures of each strain were evaluated and representative images were shown. Scale bars on the right column indicate 5  $\mu m$  which is the same for all four panels.

systems, is shown in Fig. 5. In the absence of stress, the antitoxin MqsA binds to the toxin MqsR to block its RNase activity. Furthermore, MqsA also binds to the *rpoS* promoter region via a palindrome to inhibit its transcription (Wang *et al.*, 2011). In the absence of stress, the antitoxin GhoS is produced which prevents the expression of *ghoT* by cleaving its transcript, and the translation of both proteins is coupled. Under stress, Lon protease degrades MqsA which frees the toxin MqsR (Wang *et al.*, 2011) and further induces *mqsR* expression. MqsR then degrades unprotected mRNAs primarily at 5'-GCU sites, such as *ompA* and the 5' end of *ghoST* mRNA (i.e. the coding region of *ghoS*, which contains three 5'-GCU sites). As *ghoST* is more efficiently degraded in the *ghoS* coding region, while the *ghoT* coding region stays intact, GhoT protein levels increase. This allows GhoT to exert its effects on the cell membrane, ultimately increasing persistence.

Therefore, our data further demonstrate the complexity and interconnectivity of TA systems by showing one TA system (MqsR/MqsA) may control another (GhoT/GhoS). This interconnectivity is to be expected given both the prevalence of mRNA cleavage sites of toxin RNases and their differential mRNA decay; hence, production of some proteins is facilitated during stress and this now includes preferential production of toxins via enrichment of their

mRNA. For GhoT, its production allows the cell to increase its persistence, probably by disrupting ATP generation. The physiological consequence of enrichments of other transcripts including *kilR*, *railR* and *yciG* remains to be elucidated (these genes encode a cell division inhibitor, a protein that alleviates restriction of unmodified DNA and promotes methylation, and an unknown protein respectively). Nevertheless, it is also clear now that a hierarchy of TA systems exists in the cells (e.g. MqsR/MqsA controlling GhoT/GhoS). This hierarchy was predicted (Bukowski *et al.*, 2011) and now has been demonstrated.

## Experimental procedures

### Bacterial strains, plasmids and growth conditions

The bacterial strains and plasmids are listed in Table 3. To remove the kanamycin marker for  $\Delta ghoS$  and  $\Delta ghoT$ , pCP20 was used to express the FLP recombinase (Datsenko and Wanner, 2000). To construct BW25113  $\Delta ghoS \Delta mqsRA$ , P1 transduction (Maeda *et al.*, 2008) was used to transfer the  $\Delta mqsRA$  deletion to BW25113  $\Delta ghoS$ . Luria-Bertani (LB) at 37°C was used except where indicated. Kanamycin (50  $\mu g ml^{-1}$ ) was used for pre-culturing isogenic knockout mutants and for maintaining pBS(Kan)-based plasmids, chloramphenicol (30  $\mu g ml^{-1}$ ) was used for maintaining pCA24N-based plasmids, and ampicillin (100  $\mu g ml^{-1}$ ) was used to



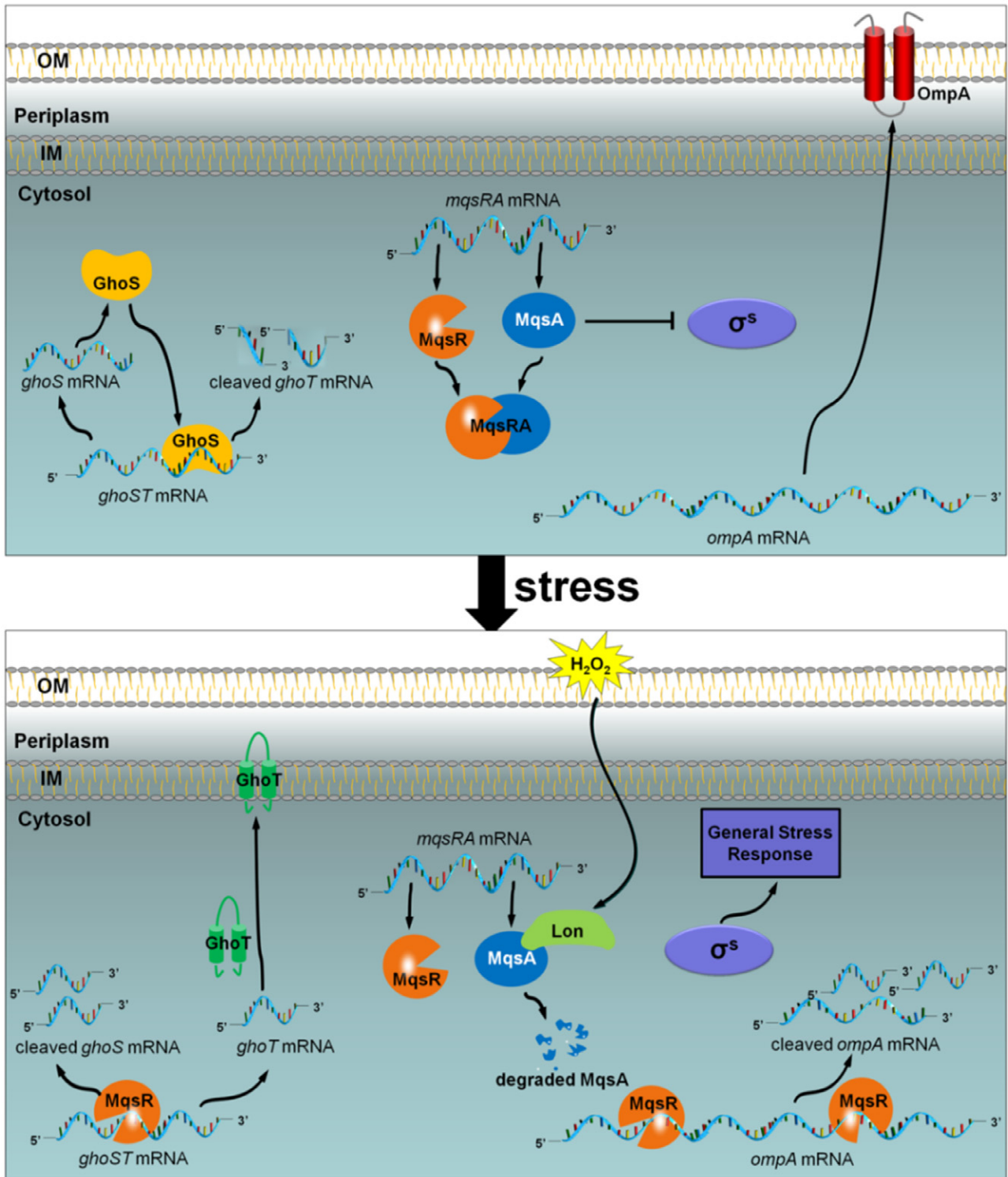


**Fig. 5.** Schematic of *MqsR*-mediated control of *GhoT/GhoS*. Without stress (upper panel), *MqsR* and *MqsA* bind and form a complex that prevents *MqsR* toxicity while *GhoS* cleaves *ghoT* mRNA to prevent *GhoT* toxicity. Upon oxidative stress (lower panel), *MqsA* is degraded by protease Lon, which derepresses *rpoS* and triggers the general stress response. The liberated *MqsR* functions as sequence-specific endoribonuclease to cleave *ghoS* mRNA, *ompA* mRNA, and other unprotected mRNAs primarily at 5'-GCU sites. As a result, *MqsR* rapidly enriches *ghoT* mRNAs which does not contain 5'-GCU sites as well as other stress-related transcripts and leads to the formation of persister cells.



**Table 3.** Bacterial strains and plasmids used in this study.

Bacterial strains/plasmids	Description	Source
<i>E. coli</i> K12 strains		
BW25113	<i>lacF</i> <sup>r</sup> <i>rrmB</i> <sub>T14</sub> $\Delta$ <i>lacZ</i> <sub>WJ16</sub> <i>hsdR514</i> $\Delta$ <i>araBAD</i> <sub>AH33</sub> $\Delta$ <i>rhaBAD</i> <sub>LD78</sub>	Baba <i>et al.</i> (2006)
BW25113 $\Delta$ <i>ghoT</i>	BW25113 $\Delta$ <i>ghoT</i> $\Omega$ Km <sup>R</sup>	Baba <i>et al.</i> (2006)
BW25113 $\Delta$ <i>ghoT</i> $\Delta$ Km	BW25113 $\Delta$ <i>ghoT</i>	This study
BW25113 $\Delta$ <i>ghoS</i>	BW25113 $\Delta$ <i>ghoS</i> $\Omega$ Km <sup>R</sup>	Baba <i>et al.</i> (2006)
BW25113 $\Delta$ <i>ghoS</i> $\Delta$ Km	BW25113 $\Delta$ <i>ghoS</i>	This study
BW25113 $\Delta$ <i>mqsRA</i>	BW25113 $\Delta$ <i>mqsRA</i> $\Omega$ Km <sup>R</sup>	Kim <i>et al.</i> (2010)
BW25113 $\Delta$ <i>ghoS</i> $\Delta$ <i>mqsRA</i>	BW25113 $\Delta$ <i>ghoS</i> $\Delta$ <i>mqsRA</i> $\Omega$ Km <sup>R</sup>	This study
Plasmids		
pCP20	Amp <sup>R</sup> & Cm <sup>R</sup> ; temperature-sensitive replication, thermal induction of FLP recombinase synthesis	Datsenko and Wanner (2000)
pCA24N	Cm <sup>R</sup> ; <i>lacF</i> , pCA24N	Kitagawa <i>et al.</i> (2005)
pCA24N- <i>mqsR</i>	Cm <sup>R</sup> ; <i>lacF</i> , pCA24N <i>P</i> <sub>T5-lac</sub> :: <i>mqsR</i> <sup>+</sup>	Kitagawa <i>et al.</i> (2005)
pCA24N- <i>ghoT</i>	Cm <sup>R</sup> ; <i>lacF</i> , pCA24N <i>P</i> <sub>T5-lac</sub> :: <i>ghoT</i> <sup>+</sup>	Kitagawa <i>et al.</i> (2005)
pCA24N- <i>ghoT-GCU</i>	Cm <sup>R</sup> ; <i>lacF</i> , pCA24N <i>P</i> <sub>T5-lac</sub> :: <i>ghoT</i> <sup>+</sup> with two 5'-GCU sites in <i>ghoT</i> mRNA	This study
pBS(Kan)	Km <sup>R</sup> ; pBS(Kan)	Canada <i>et al.</i> (2002)
pBS(Kan)- <i>mqsR</i>	Km <sup>R</sup> ; pBS(Kan) <i>P</i> <sub>lac</sub> :: <i>mqsR</i> <sup>+</sup>	Kim <i>et al.</i> (2010)
pET30a- <i>mqsR</i>	Km <sup>R</sup> ; pET30a(Kan) <i>P</i> <sub>T7</sub> :: <i>mqsR</i> <sup>+</sup>	Brown <i>et al.</i> (2012)

Chloramphenicol (30  $\mu$ g ml<sup>-1</sup>) and kanamycin (50  $\mu$ g ml<sup>-1</sup>) were used to maintain pCA24N-based plasmids and for pBS(Kan)-based plasmids, respectively, and ampicillin (100  $\mu$ g ml<sup>-1</sup>) was used to maintain plasmid pCP20.

Amp<sup>R</sup>, Cm<sup>R</sup> and Km<sup>R</sup> are ampicillin, chloramphenicol and kanamycin resistance respectively.

maintain plasmid pCP20. The persistence assay was conducted as described (Wang *et al.*, 2012) with 35 and 100  $\mu$ g ml<sup>-1</sup> ampicillin.

### Microscopy

For the measurement of the cell size after exposure to ampicillin, overnight cultures of BW25113/pCA24N, BW25113/pCA24N-*mqsR* and  $\Delta$ *ghoT*/pCA24N-*mqsR* were inoculated into LB with chloramphenicol (30  $\mu$ g ml<sup>-1</sup>) at a turbidity of 0.1, and 1 mM IPTG and ampicillin (20  $\mu$ g ml<sup>-1</sup>) were added. Cell samples were taken at 0 h, 4 h and 10 h, and washed with 0.85% NaCl. For the measurement of the cell size after exposure to ampicillin for GhoT overproduction, overnight cultures of  $\Delta$ *ghoT*/pCA24N and  $\Delta$ *ghoT*/pCA24N-*ghoT* were inoculated into LB with chloramphenicol at a turbidity of 0.1, and 1 mM IPTG was then added to induce *ghoT* expression for 2 h. Cells were washed and resuspended in LB, and ampicillin (20  $\mu$ g ml<sup>-1</sup>) was added to the cell suspension. Cell size was measured with a Zeiss Axiovert microscope with a 40 $\times$  dry objective.

To evaluate cell membrane integrity with GhoT, the Live/Dead BacLight™ Bacterial Viability Kit (Molecular Probes) was used. The kit contains SYTO 9 and propidium iodide to differentiate between cells with intact membranes (live) and cells with damaged membranes (dead). After inducing *ghoT* and *mqsR* for 3 h with 0.5 mM IPTG, BW25113  $\Delta$ *ghoT*  $\Delta$ Km/pBS(Kan)-*mqsR*/pCA24N-*ghoT* and BW25113  $\Delta$ *ghoT*  $\Delta$ Km/pBS(Kan)-*mqsR*/pCA24N-*ghoT-GCU* were harvested by centrifugation (15 000 *g*, 10 min), washed, and resuspended in 0.85% NaCl to reach a turbidity of 0.3 at 600 nm. Cells were then stained with 0.15 mM propidium iodide and 0.025 mM SYTO 9 dye for 1 h at ambient temperature. An aliquot of each cell suspension was also treated with 70% isopropyl alcohol to use as a dead cell control. Bacterial cells

were imaged using a fluorescence microscope (Zeiss Axiovert) with 40 $\times$  dry objective.

### qRT-PCR

For qRT-PCR, 50 ng of total RNA was used for qRT-PCR using the Power SYBR® Green RNA-to-C<sub>T</sub>™ 1-Step Kit and the StepOne™ Real-Time PCR System (Applied Biosystems). Primers were annealed at 60°C, and *rrsG* (Wang *et al.*, 2009) was used to normalize the data.

### Site-directed mutagenesis

Site-directed mutagenesis (Wang *et al.*, 2011) was used to introduce two 5'-GCU sites into the coding region of *ghoT* in pCA24N-*ghoT* to create pCA24N-*ghoT-GCU* (Fig. 2) using two primer pairs, GhoT-GCU-1 and GhoT-GCU-2 respectively (Table 1). DNA sequencing using the BigDye Terminator Cycle Sequencing kit was performed to confirm the targeted mutations at these sites.

### *MqsR* endoribonuclease assay

Refolding and purification of MqsR was performed as described (Brown *et al.*, 2012) after producing MqsR from pET30a-*mqsR*. For the synthesis of *ghoS*, *ghoT* and *ghoT-GCU* mRNAs, PCR products were obtained using the primers shown in Table 1 and were used as templates for *in vitro* transcription with T7 RNA polymerase. The T7 RNA polymerase promoter sequence was included in the forward primers. PCR products were purified using the PureLink PCR purification kit (Invitrogen), and 1  $\mu$ g of the PCR product was used as the template for the *in vitro* RNA reaction with the AmpliScribe T7-Flash transcription kit (Epicentre). The reaction

mixture for the MqsR endoribonuclease cleavage assay (10  $\mu$ l) contained 2  $\mu$ g of mRNA, 100 mM KCl, 2.5 mM MgCl<sub>2</sub>, and either 30 ng of purified MqsR protein in MqsR buffer (10 mM Tris pH 7.5, 100 mM NaCl, 0.5 mM TCEP) or an equivalent volume of MqsR buffer (for those reaction without MqsR protein). The reaction mixture was incubated at 37°C for 15 min and quenched by the addition of an equal volume of 2 $\times$  sample loading buffer (Invitrogen). The reaction products were resolved by electrophoresis with RNA denaturing gels (15% polyacrylamide with 7 M urea, Invitrogen).

### Acknowledgements

This work was supported by the NIH (R01 GM089999 to T.W.), the NSF (CAREER award MCB 0952550 to R.P.), the NSFC (31270214 to X.W.) and the 1000-Youth Elite Program from China (to X.W.). We are grateful for the Keio and ASKA strains provided by the Genome Analysis Project in Japan and for the help of Brian Kwan with a persistence assay. T.W. is the Biotechnology Endowed Professor at the Pennsylvania State University.

### References

- Amitai, S., Kolodkin-Gal, I., Hananya-Meltabashi, M., Sacher, A., and Engelberg-Kulka, H. (2009) *Escherichia coli* MazF leads to the simultaneous selective synthesis of both 'death proteins' and 'survival proteins'. *PLoS Genet* **5**: e1000390.
- Baba, T., Ara, T., Hasegawa, M., Takai, Y., Okumura, Y., Baba, M., *et al.* (2006) Construction of *Escherichia coli* K-12 in-frame, single-gene knockout mutants: the Keio collection. *Mol Syst Biol* **2**: 2006.0008.
- Balaban, N.Q., Merrin, J., Chait, R., Kowalik, L., and Leibler, S. (2004) Bacterial persistence as a phenotypic switch. *Science* **305**: 1622–1625.
- Brown, B.L., Wood, T.K., Peti, W., and Page, R. (2011) Structure of the *Escherichia coli* antitoxin MqsA (YgiT/b3021) bound to its gene promoter reveals extensive domain rearrangements and the specificity of transcriptional regulation. *J Biol Chem* **286**: 2285–2296.
- Brown, B.L., Lord, D.M., Grigoriu, S., Peti, W., and Page, R. (2012) The *E. coli* toxin MqsR destabilizes the transcriptional repression complex formed between the antitoxin MqsA and the *mqsRA* operon promoter. *J Biol Chem* doi: 10.1074/jbc.M112.421008.
- Bukowski, M., Rojowska, A., and Wladyka, B. (2011) Prokaryotic toxin–antitoxin systems – the role in bacterial physiology and application in molecular biology. *Acta Biochim Pol* **58**: 1–9.
- Canada, K.A., Iwashita, S., Shim, H., and Wood, T.K. (2002) Directed evolution of toluene *ortho*-monooxygenase for enhanced 1-naphthol synthesis and chlorinated ethene degradation. *J Bacteriol* **184**: 344–349.
- Christensen-Dalsgaard, M., Jørgensen, M.G., and Gerdes, K. (2010) Three new RelE-homologous mRNA interferases of *Escherichia coli* differentially induced by environmental stresses. *Mol Microbiol* **75**: 333–348.
- Datsenko, K.A., and Wanner, B.L. (2000) One-step inactivation of chromosomal genes in *Escherichia coli* K-12 using PCR products. *Proc Natl Acad Sci USA* **97**: 6640–6645.
- Domka, J., Lee, J., Bansal, T., and Wood, T.K. (2007) Temporal gene-expression in *Escherichia coli* K-12 biofilms. *Environ Microbiol* **9**: 332–346.
- Donachie, W.D., and Begg, K.J. (1970) Growth of the bacterial cell. *Nature* **227**: 1220–1224.
- Dörr, T., Vulić, M., and Lewis, K. (2010) Ciprofloxacin causes persister formation by inducing the TisB toxin in *Escherichia coli*. *PLoS Biol* **8**: e1000317.
- González Barrios, A.F., Zuo, R., Hashimoto, Y., Yang, L., Bentley, W.E., and Wood, T.K. (2006) Autoinducer 2 controls biofilm formation in *Escherichia coli* through a novel motility quorum-sensing regulator (MqsR, B3022). *J Bacteriol* **188**: 305–316.
- Hayes, F., and Van Melderen, L. (2011) Toxins–antitoxins: diversity, evolution and function. *Crit Rev Biochem Mol Biol* **46**: 386–408.
- Hu, Y., Benedik, M.J., and Wood, T.K. (2012) Antitoxin DinJ influences the general stress response through transcript stabilizer CspE. *Environ Microbiol* **14**: 669–679.
- Hurley, J.M., Cruz, J.W., Ouyang, M., and Woychik, N.A. (2011) Bacterial toxin RelE mediates frequent codon-independent mRNA cleavage from the 5' end of coding regions *in vivo*. *J Biol Chem* **286**: 14770–14778.
- Keren, I., Shah, D., Spoering, A., Kaldalu, N., and Lewis, K. (2004) Specialized persister cells and the mechanism of multidrug tolerance in *Escherichia coli*. *J Bacteriol* **186**: 8172–8180.
- Kim, Y., and Wood, T.K. (2010) Toxins Hha and CspD and small RNA regulator Hfq are involved in persister cell formation through MqsR in *Escherichia coli*. *Biochem Biophys Res Commun* **391**: 209–213.
- Kim, Y., Wang, X., Zhang, X.-S., Grigoriu, S., Page, R., Peti, W., and Wood, T.K. (2010) *Escherichia coli* toxin/antitoxin pair MqsR/MqsA regulate toxin CspD. *Environ Microbiol* **12**: 1105–1121.
- Kitagawa, M., Ara, T., Arifuzzaman, M., Ioka-Nakamichi, T., Inamoto, E., Toyonaga, H., and Mori, H. (2005) Complete set of ORF clones of *Escherichia coli* ASKA library (a complete set of *E. coli* K-12 ORF archive): unique resources for biological research. *DNA Res* **12**: 291–299.
- Lewis, K. (2007) Persister cells, dormancy and infectious disease. *Nat Rev Microbiol* **5**: 48–56.
- Lewis, K. (2010) Persister cells. *Annu Rev Microbiol* **64**: 357–372.
- Maeda, T., Sanchez-Torres, V., and Wood, T.K. (2008) Metabolic engineering to enhance bacterial hydrogen production. *Microb Biotechnol* **1**: 30–39.
- Maisonneuve, E., Shakespeare, L.J., Jørgensen, M.G., and Gerdes, K. (2012) Bacterial persistence by RNA endonucleases. *Proc Natl Acad Sci USA* **108**: 13206–13211.
- Masuda, H., Tan, Q., Awano, N., Wu, K., and P., and Inouye, M. (2012) YeeU enhances the bundling of cytoskeletal polymers of MreB and FtsZ, antagonizing the CbtA (YeeV) toxicity in *Escherichia coli*. *Mol Microbiol* **84**: 979–989.
- Pecota, D.C., and Wood, T.K. (1996) Exclusion of T4 phage by the *hok/sok* killer locus from plasmid R1. *J Bacteriol* **178**: 2044–2050.
- Pfaffl, M.W. (2001) A new mathematical model for relative quantification in real-time RT-PCR. *Nucleic Acids Res* **29**: e45.

- Ren, D., Bedzyk, L.A., Thomas, S.M., Ye, R.W., and Wood, T.K. (2004) Gene expression in *Escherichia coli* biofilms. *Appl Microbiol Biotechnol* **64**: 515–524.
- Rolinson, G.N. (1980) Effect of beta-lactam antibiotics on bacterial cell growth rate. *J Gen Microbiol* **120**: 317–323.
- Shah, D., Zhang, Z., Khodursky, A., Kaldalu, N., Kurg, K., and Lewis, K. (2006) Persisters: a distinct physiological state of *E. coli*. *BMC Microbiol* **6**: 53.
- Staugaard, P., van den Berg, F.M., Woldringh, C.L., and Nanninga, N. (1976) Localization of ampicillin-sensitive sites in *Escherichia coli* by electron microscopy. *J Bacteriol* **127**: 1376–1381.
- Wang, X., and Wood, T.K. (2011) Toxin/antitoxin systems influence biofilm and persister cell formation and the general stress response. *Appl Environ Microbiol* **77**: 5577–5583.
- Wang, X., Kim, Y., and Wood, T.K. (2009) Control and benefits of CP4-57 prophage excision in *Escherichia coli* biofilms. *ISME J* **3**: 1164–1179.
- Wang, X., Kim, Y., Hong, S.H., Ma, Q., Brown, B.L., Pu, M., et al. (2011) Antitoxin MqsA helps mediate the bacterial general stress response. *Nat Chem Biol* **7**: 359–366.
- Wang, X., Lord, D.M., Cheng, H.-Y., Osbourne, D.O., Hong, S.H., Sanchez-Torres, V., et al. (2012) A new type V toxin–antitoxin system where mRNA for toxin GhoT is cleaved by antitoxin GhoS. *Nat Chem Biol* **8**: 855–861.
- Yamaguchi, Y., Park, J.-H., and Inouye, M. (2009) MqsR, a crucial regulator for quorum sensing and biofilm formation, is a GCU-specific mRNA interferase in *Escherichia coli*. *J Biol Chem* **284**: 28746–28753.